Possible Pairing Symmetry of Three-dimensional Superconductor UPt_3
— Analysis Based on a Microscopic Calculation —

Shogo SHINKAI* and Kosaku YAMADA

Depertment of Physics, Kyoto University, Sakyo-ku, Kyoto 606-8502

(Received February 2, 2008)

Stimulated by the anomalous superconducting properties of UPt_3, we investigate the pairing symmetry and the transition temperature in the two-dimensional(2D) and three-dimensional(3D) hexagonal Hubbard model. We solve the Éliashberg equation using the third order perturbation theory with respect to the on-site repulsion U. As results of the 2D calculation, we obtain distinct two types of stable spin-triplet pairing states. One is the f-wave(B_1) pairing around $n = 1.2$ and in a small U region, which is caused by the ferromagnetic fluctuation. Then, the other is the p_x(or p_y)-wave(E_1) pairing in large U region far from the half-filling ($n = 1$) which is caused by the vertex corrections only. However, we find that the former f-wave pairing is destroyed by introduced 3D dispersion. This is because the 3D dispersion breaks the favorable structures for the f-wave pairing such as the van Hove singularities and the small pocket structures. Thus, we conclude that the ferromagnetic fluctuation mediated spin-triplet state can not explain the superconductivity of UPt_3. We also study the case of the pairing symmetry with a polar gap. This p_z-wave(A_1) is stabilized by the large hopping integral along c-axis t_z. It is nearly degenerate with the suppressed p_x(or p_y)-wave(E_1) in the best fitting parameter region to UPt_3 ($1.3 \leq t_z \leq 1.5$). These two p-wave pairing states exist in the region far from the half-filling, in which the vertex correction terms play crucial roles like the case in Sr_2RuO_4.

KEYWORDS: UPt_3, third-order perturbation theory, spin-triplet superconductivity, heavy fermion

1. Introduction

Much attention have been focused on hexagonal heavy fermion superconductor UPt_3, since it was discovered in 1984.[1] The heavy fermion state is characterized by its large value of the electronic specific heat coefficient $\gamma = 420\text{mJ/K}^2\text{moleU}$. The coefficient of T^2-law of resistivity is also enhanced by 10^5 times as large as that of conventional metal. Such behavior arises from the strong electron correlation. In UPt_3, the itinerant electrons compose such a Fermi liquid state and then undergo superconducting transition. In zero field, the two superconducting transitions occur at $\sim$0.48 K and $\sim$0.52 K.[2,3] The field-temperature phase diagram was constructed experimentally[4] and it consists of at least three phases (denoted as A, B and C). Most of theoretical models for this splitting of T_c are based on the coupling

between the superconducting order parameter and the small antiferromagnetic moment ($\mu_S = 0.02\mu_B$/U) which appears below $T_N \sim 5\text{K}$[5].[6]

Furthermore, a power law behavior of the ultrasound attenuation,[7] NMR relaxation rate,[8] specific heat[23] and penetration depth[9] below T_c suggested an unusual order parameter with energy gap which vanishes at some points on the Fermi surface. In addition, the NMR[810] and muon spin rotation-relaxation (μSR)[11] experiments detected no change of the Knight shift below T_c. These suggest a possibility of the odd-parity of the Cooper pairing.

In order to explain these unconventional properties in UPt$_3$, various phenomenological theories have been proposed. Theories based on two-dimensional representation[1213] assign a gap with both point nodes along c-axis and a line of nodes at $k_z = 0$ (called a hybrid gap) to the phase B. On the other hand, the theory based on one-dimensional representation[14] requires either a hybrid gap or a gap with only a line of nodes at $k_z = 0$ (a polar gap). The experiments of thermal conductivity[1516] and penetration depth[9] suggested that a hybrid gap is favored, but the gap structure of UPt$_3$ has not been completely determined.

In contrast with the phenomenological theories, few microscopical theories determining the pairing symmetry and the gap structure have been reported. The band calculations[1718],[19] based on the assumption that 5f-electrons are itinerant, reported that five three-dimensional bands form the Fermi surface. The results of the de Haas-van Alphen (dHvA) experiments[211920] are consistent with these band calculations, and the observed effective mass of each band is almost 20 times as large as the corresponding calculated mass. Among these five bands, we take up band 37-electron in ref.19 (a rugby ball like band structure with small electron pockets at K-points in the hexagonal Brillouin zone) because it has the heaviest effective mass and occupies the largest area of the Fermi surface. Then, in the following sections, we discuss the pairing symmetry in the microscopic way based on band 37-electron.

2. Model

We consider the following single band Hubbard model on hexagonal lattice,

$$H = H_0 + H_{\text{int}}, \tag{1}$$

$$H_0 = \sum_{\vec{k}\sigma} \xi(\vec{k}) c_{\vec{k}\sigma}^{\dagger} c_{\vec{k}\sigma}, \tag{2}$$

$$H_{\text{int}} = \frac{U}{2N} \sum_{\vec{k}_i} \sum_{\sigma \neq \sigma'} \delta_{\vec{k}_1+\vec{k}_2,\vec{k}_3+\vec{k}_4} c_{\vec{k}_1\sigma}^{\dagger} c_{\vec{k}_2\sigma'}^{\dagger} c_{\vec{k}_3\sigma'} c_{\vec{k}_4\sigma}. \tag{3}$$

From the tight binding approximation, energy dispersion $\xi(\vec{k})$ is given by

$$\xi(\vec{k}) = -2t_1 \left(2\cos\frac{\sqrt{3}k_x}{2}\cos\frac{k_y}{2} + \cos k_y \right)$$

$$-2t_2 \left(\cos\sqrt{3}k_x + 2\cos\frac{\sqrt{3}k_x}{2}\cos\frac{3k_y}{2} \right)$$

$$- 2t_3 \left(2 \cos \sqrt{3} k_x \cos k_y + \cos 2k_y \right)$$

$$- 2t_z \left(\cos k_z \right) - \mu. \tag{4}$$

Here, t_1, t_2 and t_3 are the nearest-, the next-nearest-, and the third-nearest-neighbor hopping integrals in ab-plane respectively. The t_z is the hopping integral along c-axis, and μ is the chemical potential. Now we fix $t_1 = 1$, and calculate physical quantities changing the other variables t_2, t_3, t_z, U and electron filling n.

3. Formulation

One of the authors (K.Y.) has described the Fermi liquid theory for the heavy electron system[22].[23] Based on this idea, we start from the renormalized quasiparticle state, and calculate the momentum dependence of the effective interaction between them.

Recently, some authors have calculated the transition temperture T_c and the pairing symmetry for many superconductors including high-T_c cuprates and Sr_2RuO_4 on the basis of the third order perturbation theory (TOPT) with respect to U.[24] All of them are in good agreement with experimental facts. Although the convergence of the vertex correction terms is an important problem, TOPT in the moderately correlated region has been justified by higher order calculations.[25] Thus, in the same framework, we apply TOPT to our model.

In TOPT, the effective interaction for the spin-singlet state is given by

$$V^S(k, k') = V^S_{RPA}(k, k') + V^S_{Vertex}(k, k') \tag{5}$$

$$V^S_{RPA}(k, k') = U + U^2 \chi_0(k - k') + 2U^3 \chi_0^2(k - k') \tag{6}$$

$$V^S_{Vertex}(k, k') = 2U^3 \mathrm{Re} \left[\sum_q G(k + q) G(k' + q) [\chi_0(q) - \phi_0(q)] \right]. \tag{7}$$

For the spin-triplet state,

$$V^T(k, k') = V^T_{RPA}(k, k') + V^T_{Vertex}(k, k') \tag{8}$$

$$V^T_{RPA}(k, k') = -U^2 \chi_0(k - k') \tag{9}$$

$$V^T_{Vertex}(k, k') = 2U^3 \mathrm{Re} \left[\sum_q G(k + q) G(k' + q) [\chi_0(q) + \phi_0(q)] \right], \tag{10}$$

where

$$\chi_0(q) = -\sum_k G(k + q) G(k) \tag{11}$$

$$\phi_0(q) = -\sum_k G(q - k) G(k) \tag{12}$$

$$G(k) = \frac{1}{i\omega_n - \xi(\vec{k})}. \tag{13}$$

Here, k is a shorthand notation as $k = (\vec{k}, i\omega_n)$ and $\omega_n = \pi T(2n + 1)$ is a fermion Matsubara frequency. $\xi(\vec{k})$ is the band of quasiparticles with large effective mass. In Fig.1, the diagrams
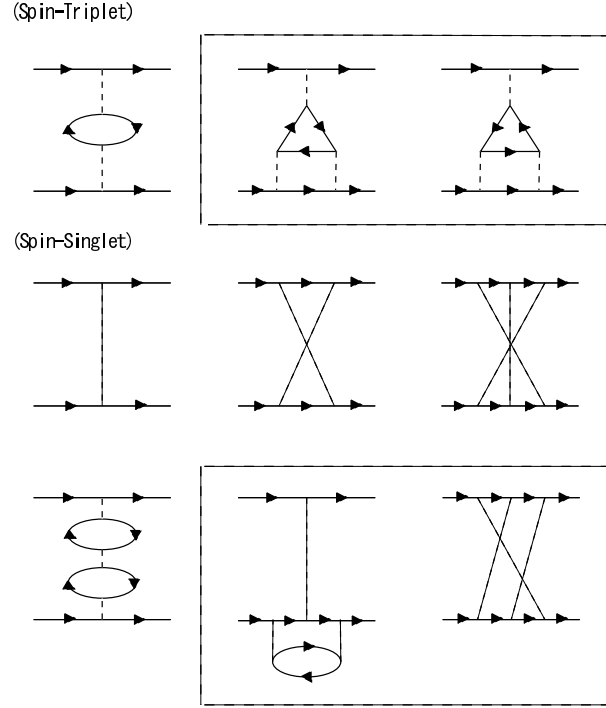
Fig. 1. Feynman diagrams of the effective interaction up to third order. Solid and dashed lines correspond to the Green's function and the interaction, respectively.

of the effective interaction are shown. The diagrams enclosed by a dashed line are the vertex correction terms. We calculate T_c and the pairing symmetry by solving the Éliashberg equation,

$$\lambda_{\max}\Delta(k) = -\frac{T}{N}\sum_{k'}V(k,k')|G(k')|^2\Delta(k'). \tag{14}$$

At $T = T_c$, the maximum eigenvalue $\lambda_{\max}$ becomes unity, and the pairing symmetry is determined by the momentum dependence of the gap function $\Delta(k)$. Thus, by estimating $\lambda_{\max}$, we can determine which type of pairing symmetry is stable. Here, we have ignored the damping effect due to the normal selfenergy. This contribution is important for estimating T_c quantitatively, but qualitative properties of superconductivity such as the pairing symmetry is not usually influenced.

4. Results of 2D Calculations

In this section, we show the results of two-dimensional calculations, considering the $k_z = 0$ plane (including Γ, K, M points in the hexagonal Brillouin zone) of the band 37, that is, we fix $t_z = 0$. Here, we notice that band 37 is highly three-dimensional, but the calculations on the basal triangular lattice gives us much information as starting points. We will show the results of 3D calculations by introducing t_z in §5. Then, we also fix $t_3 = 0$ and $T = 0.01$ in this section. The calculated Fermi surfaces are shown in Fig.2. We can see larger electron pockets
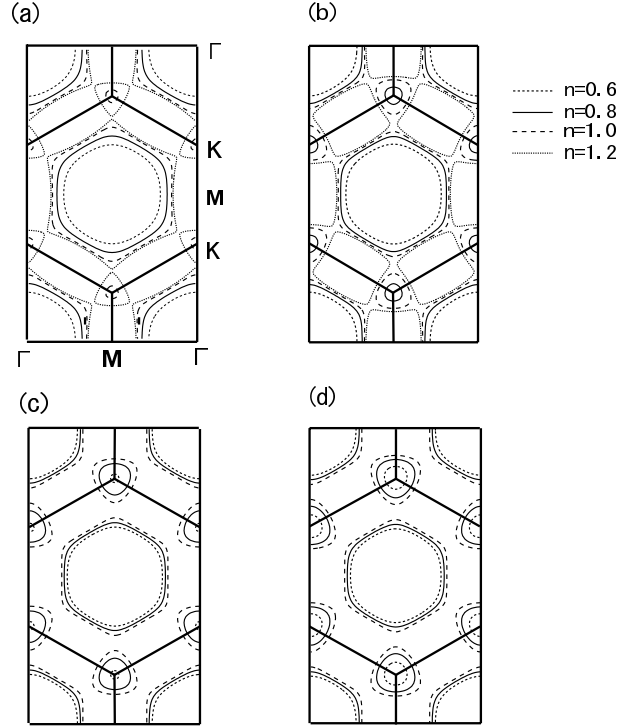
Fig. 2. Calculated Fermi surfaces in the case of (a)$t_2 = 0.3$, $n = 0.6, 0.8, 1.0, 1.2$ (b)$t_2 = 0.4$, $n = 0.6, 0.8, 1.0, 1.2$ (c)$t_2 = 0.5$, $n = 0.6, 0.8, 1.0$ (d)$t_2 = 0.6$, $n = 0.6, 0.8, 1.0$. Electron pockets at K-points become large as either n or t_2 increases.

at K-points as either n or t_2 increases. Within the $k_z = 0$ plane, the best fitting parameter region for UPt$_3$ is $t_2 = 0.4 \sim 0.6$, $n = 0.7 \sim 1.0$. The possible candidate of pairing symmetry in 2D triangular lattice belongs to the following irreducible representations of C_{6v}.

symmetry	One of basis function
B$_1$(f_1-wave)	$\sin \frac{k_y}{2} \left(\cos \frac{\sqrt{3}k_x}{2} - \cos \frac{k_y}{2} \right)$
B$_2$(f_2-wave)	$\sin \frac{\sqrt{3}k_x}{2} \left(\cos \frac{\sqrt{3}k_x}{2} - \cos \frac{3k_y}{2} \right)$
E$_1$(p-wave)	$\begin{cases} \sin \frac{\sqrt{3}k_x}{2} \cos \frac{k_y}{2} \\ \cos \frac{\sqrt{3}k_x}{2} \sin \frac{k_y}{2} + \sin k_y \end{cases}$
E$_2$(d-wave)	$\begin{cases} \sin \frac{\sqrt{3}k_x}{2} \sin \frac{k_y}{2} \\ \cos \frac{\sqrt{3}k_x}{2} \cos \frac{k_y}{2} - \cos k_y \end{cases}$

First, we set $U = 2$. Figure 3 is a contour plot of $\lambda_{\max}$ as a function of t_2 and electron filling n ($n = 1$ at the half filling). The black thick line represents the crossover line of two pairing symmetries. When n is larger than half filling, an f_1(B$_1$)-wave spin-triplet state is stable. This f_1-wave state was predicted by Ikeda *et al.*[26] in the case of Na$_x$CoO$_2 \cdot y$H$_2$O. In contrast, for the case less than half filling, d(E$_2$)-wave pairing state covers a wide region. But the eigenvalues of this d-wave state is too low to be realized. Then, what is the origin of f-wave pairing above half filling? In figure 4, we show the bare spin susceptibility $\chi_0(\vec{q}, 0)$ in
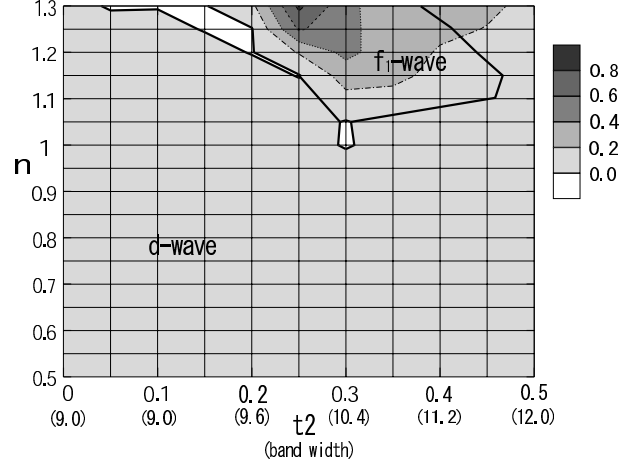
Fig. 3. The contour plot of $\lambda_{\max}$ as a function of t_2 (band width) and n in the case of $U = 2$ and $T = 0.01$. An f_1-wave spin-triplet state is stable in the large n region. The eigenvalue for d-wave pairing below the half filling is too low to be realized.

the case of $t_2 = 0.3, n = 1.2$. The peak structures can be seen at Γ-points, and cannot be seen in the region where d-wave pairing state is stable. This peak corresponds to the increase of the density of states by van Hove singularity, which can be seen around K-point in Fig.2(a) (n=1.2). The peak structure at Γ-point implies the ferromagnetic instability. These conditions stabilize the f_1-wave triplet pairing. Next, to examine influence of the vertex corrections, we calculate the eigenvalues by including only the RPA-like diagrams of the effective interaction up to the third order. The n-dependence of the calculated eigenvalues for f_1-wave pairing in the RPA-like calculation, and that for f_1- and d-wave in TOPT are shown in Fig.5. We can see the vertex correction terms work in favor of realizing the triplet pairing, as Nomura $et\ al.$ predicted in Sr_2RuO_4.[25] Here, we have to note that the Fermi surface in this f_1-wave region is rather larger than actual one. This does not continue to the best fitting region for UPt_3 ($t_2 = 0.4 \sim 0.6, n = 0.7 \sim 1.0$), because of the absence of the van Hove singularities near the Fermi surface in spite of the existence of the electron pockets.

Next, we set $U = 5$ to investigate the triplet pairing in the best fitting parameter region. Figure 6 is a contour plot of $\lambda_{\max}$ as a function of t_2 and n. We can see $p(E_1)$-wave spin-triplet pairing state appears in low n region. In this region, there are no significant peak structures at Γ-point, because van Hove singularities and/or small pocket structures are lacking. Thus, this p-wave pairing is caused by the vertex correction only, in contrast with the previous f-wave pairing. Then we increase U to $U = 7$, and show a contour plot of $\lambda_{\max}$ as a function of t_2 and n in Fig.7. We can see the p-wave pairing becomes stable. Far from the half-filling, the p-wave pairing covers a wide region which includes the best fitting parameter region for UPt_3. Here, we note, in the case of $n \geq 0.9$ for large U, we cannot perform reliable calculations because U maybe too large compared with $1/\chi_0^{\max}$, where $1/\chi_0^{\max}$ is the maximum value of the bare
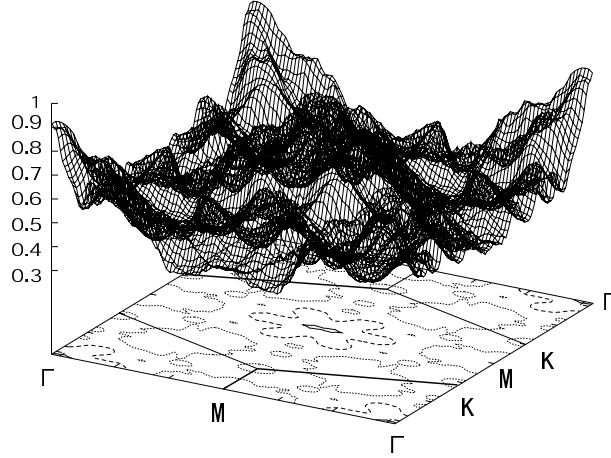
Fig. 4. The bare spin susceptibility $\chi_0(\vec{q}, 0)$ in the case of $t_2 = 0.3$, $n = 1.2$ and $T = 0.01$. We can see peak structures around Γ-points.
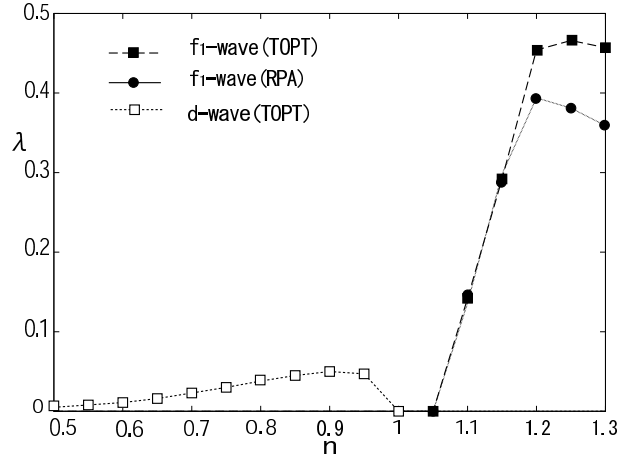

Fig. 5. The n-dependence of eigenvalues in the case of $t_2 = 0.3$, $U = 2$ and $T = 0.01$. The dashed (dotted) line with black (white) squares is the result for f_1-wave (d-wave) pairing in TOPT. The line with black circles is the result for f_1-wave pairing in the RPA-like calculation.

susceptibility $\chi_0(\vec{q}, 0)$.

In this section, we have obtained distinct two types of stable triplet pairing states. One is the $f(\mathrm{B}_1)$-wave pairing in large n and small U region, which is caused by the ferromagnetic fluctuation. The vertex correction terms also increase $\lambda_{\max}$ for this f-wave pairing. Another is the $p(\mathrm{E}_1)$-wave pairing in large U region far from the half filling. This state is caused by the vertex corrections only, but the form of the Fermi surface is in better agreement with that from the band calculations. However, since the band 37 is highly three-dimensional, we have to introduce 3D dispersion and investigate the stability for the effect of three-dimensionality.
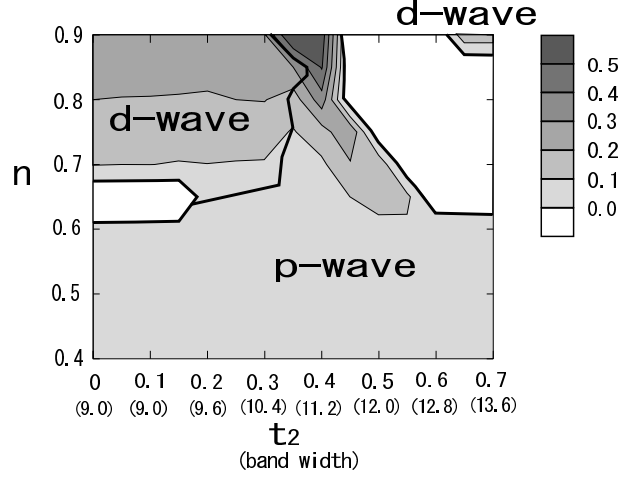
Fig. 6. The contour plot of $\lambda_{\max}$ as a function of t_2 (band width) and n in the case of $U = 5$ and $T = 0.01$. Here, we consider the case of less than half-filling only. A p-wave pairing appears far from the half-filling.
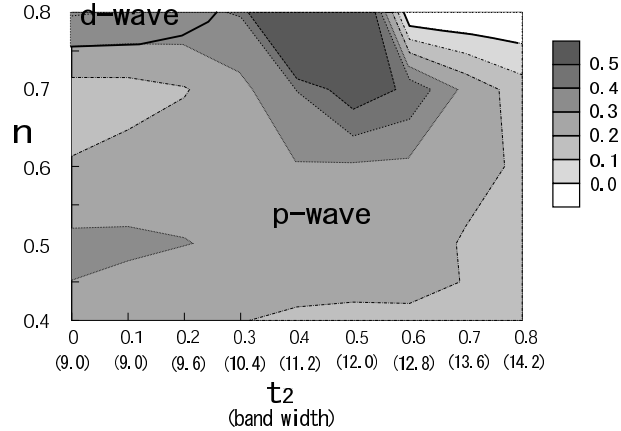

Fig. 7. The contour plot of $\lambda_{\max}$ as a function of t_2 (band width) and n in the case of $U = 7$ and $T = 0.01$. A p-wave triplet pairing is stabilized by the vertex corrections for large U, and covers the wide region.

5. Results of 3D Calculations

5.1 Stability for 3D dispersion

In this section, we investivate the effect of 3D dispersion on these two pairing states, introducing t_z. We also fix $t_3 = 0$ and $T = 0.01$ in this section. First, we apply the 3D calculation to the high-filling $f_1(B_1)$-wave pairing state at $U = 2$. In Fig.8, we show the t_z-dependence of eigenvalues for f_1-wave state in two cases $t_2 = 0.3, n = 1.2$ and $t_2 = 0.3, n = 1.15$. As t_z increases, the eigenvalues show relatively sharp decrease (compared with the next p-wave cases) and then vanishes near $t_z = 0.3$. This result is different from the case of d-wave pairing on the square lattice:[27] In that case T_c begins to be suppressed at $t_z = 0.4$,
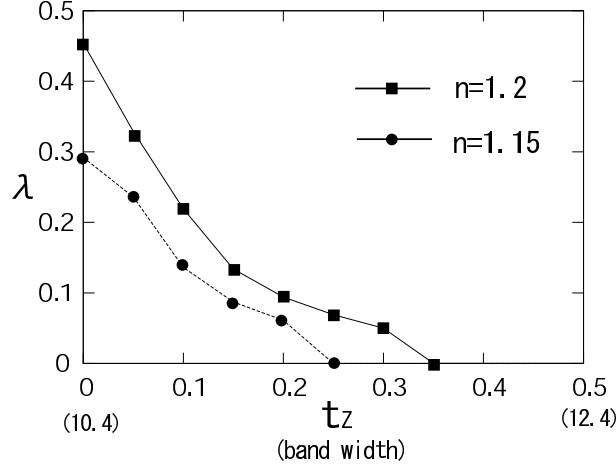
Fig. 8.   The t_z-dependence of eigenvalues for $f_1(B_1)$-wave pairing in the case of $t_2 = 0.3$, $U = 2$ and $T = 0.01$. The line with black squares (circles) is the result for $n = 1.2$ ($n = 1.15$) in TOPT. The suppression of $\lambda_{\max}$ by 3D dispersion is very strong.

then decreases by one order of magnitude at $t_z = 1.0$. In our case, the rapid decrease of the eigenvalue for f_1-wave indicates that the ferromagnetic fluctuation mediated spin-triplet superconductivity is easily destroyed by three-dimensionality, which breaks both the van Hove singularities and the small pocket structures. Actually, the band 37 is highly three-dimensional ($t_z \geq 1$) and both structures exist only near the $k_z = 0$ plane. Thus, we conclude that this f_1-wave pairing can not explain the superconductivity of UPt$_3$.

Next, we apply the 3D dispersion to the low-filling $p(E_1)$-wave state at $U = 7$. In Fig.9, we show the t_z-dependence of eigenvalues for p-wave state in the two cases $t_2 = 0.4, n = 0.6$ and $t_2 = 0.4, n = 0.7$. In contrast to the f_1-wave pairing case, the decrease of the eigenvalue of the p-wave pairing is rather slow, especially far from the half-filling. This is because the p-wave pairing is not caused by the special structures of Fermi surface but the vertex corrections. When we introduce t_z, the calculated band width become larger. Thus we increase the on-site repulsion U and try to obtain the reliable eigenvalues in the next subsection.

5.2   Pairing Symmetry with a Polar Gap

There are many pairing symmetries in hexagonal lattice (D_{6h}) in addition to the irreducible representations of C_{6v}, for example $E_{1g}(d_{xz}$ and d_{yz} are degenerated), $E_{2g}(d_{xy}$ and $d_{x^2-y^2}$ are degenerated), $B_{1g}(g$-wave), $B_{2g}(g$-wave) for spin-singlet state, $A_{1u}(p_z)$, $E_{1u}(p_x$ and p_y are degenerated), $E_{2u}(f_{xyz}$ and $f_{(x^2-y^2)z}$ are degenerated), $B_{1u}(f_1)$, $B_{2u}(f_2)$ for spin-triplet state.

In this section, we investigate $\lambda_{\max}$ using 3D band structure from beginning. Calculated Fermi surface in the case of $t_2 = 0.3$, $t_3 = -0.5$, $n = 0.45$ and $t_z = 1.4$ is shown in Fig.10. This well describes the band 37-electron. Such a low electron filling ($n = 0.45$) is due to the absence of electron in $k_z = \pm\pi$ plane. In Fig.11, we show the U-dependence of positive eigenvalues at
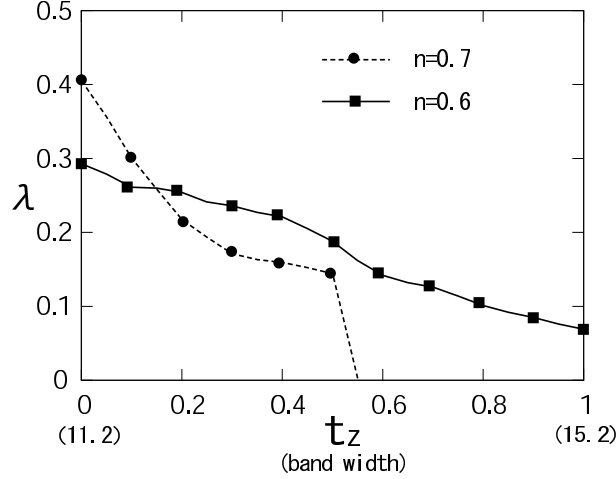
Fig. 9.   The t_z-dependence of eigenvalues for $p(E_1)$-wave pairing in the case of $t_2 = 0.4$, $U = 7$ and $T = 0.01$. The solid (dashed) line with black squares (circles) is the result for $n = 0.6$ ($n = 0.7$) in TOPT. This low-filling p-wave pairing is stable for 3D dispersion compared with the f_1-wave in Fig.8.

$T = 0.01$. Because we consider the region far from the half-filling, the d-wave pairing states are suppressed by the large vertex corrections from large U. On the other hand, the p-wave pairings are stabilized by them. The two p-wave pairing (A$_{1u}$ and E$_{1u}$) are nearly degenerate, and the stable state between them is changed by the small variations of some other parameters such as t_2, t_3, n and t_z. Thus it is difficult for us to determine which p-wave pairing is stable. Here, we note that the band width in this parameter equals 16.0, which is much larger than that in 2D calculations, thus such large value of U in Fig.11 is usable. Next, in Fig.12, we show the t_z-dependence of eigenvalues for $p_x(E_{1u})$-wave and $p_z(A_{1u})$-wave pairing states at $U = 9$ and $T = 0.01$. The eigenvalue for $p_x(E_{1u})$-wave pairing is suppressed by 3D dispersion t_z as shown in §5.1. On the other hand, $p_z(A_{1u})$-wave pairing is stabilized by t_z. These two p-wave states are nearly degenerate in the best fitting parameter region to UPt$_3$ ($1.3 \leq t_z \leq 1.5$). The $p_z(A_{1u})$-wave pairing agrees with experimental results which confirm the gap structure with a line of nodes at $k_z = 0$ plane. However, we cannot explain the E$_{2u}$ hybrid gap (f_{xyz} and $f_{(x^2-y^2)z}$). We may have to use more realistic models such as a multi-orbital model to explain it.

6.   Discussions

In this paper, we have investigated the single band Hubbard model for UPt$_3$ on the basis of the perturbation theory. We have performed all the calculations in renormalized scheme, where we consider $\xi(\vec{k})$ to be the dispersion of quasiparticles with heavy effective mass. In that scheme, we should not include the normal selfenergy corrections giving rise to mass enhancement which has been already included by the renormalization. Therefore we
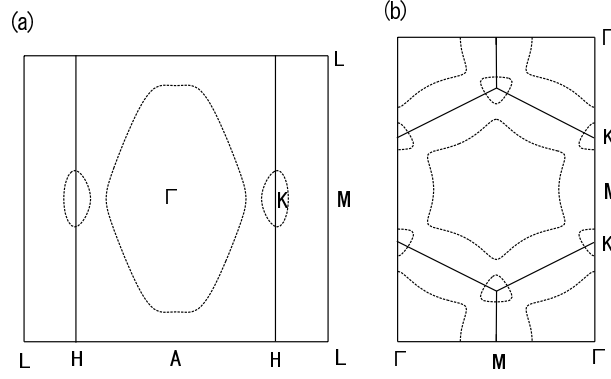
Fig. 10.   The Fermi surface at $t_2 = 0.3$, $t_3 = -0.5$, $n = 0.45$ and $t_z = 1.4$ (a)in $k_y = 0$ plane, (b)in $k_z = 0$ plane. This well describes the band 37-electron in ref.19.
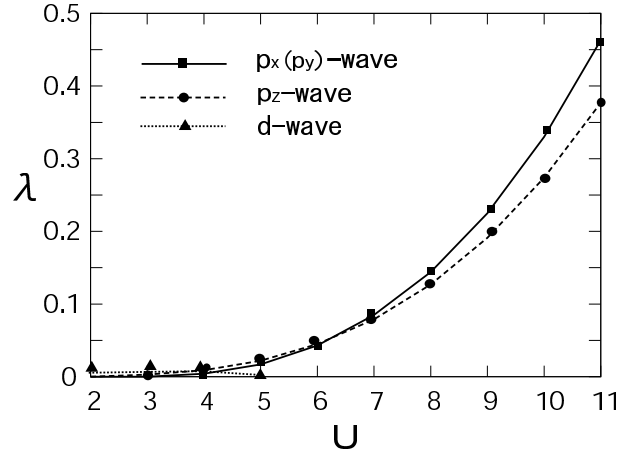

Fig. 11.   The U-dependence of eigenvalues for p_z-wave (A_{1u}) pairing and $p_x(p_y)$-wave (E_{1u}) pairing in the case of $t_2 = 0.3$, $t_3 = -0.5$, $n = 0.45$, $t_z = 1.4$ and $T = 0.01$. The band width is 16.0. The solid (dashed) line with black squares (circles) is the result for p_x-wave (p_z-wave) in TOPT, and the dotted line with black triangles is the result for $d_{xy}(d_{x^2-y^2})$-wave (E_{2g}). In large U region, two p-wave pairings are stabilized by the vertex corrections, and these are nearly degenerate.

have ignored them. As a result, we have also ignored the damping effect due to the normal selfenergy, but qualitative properties of superconductivity such as the pairing symmetry is not usually influenced.[24]

When we examine T_c quantitatively, we have to estimate the band width of the heavy quasiparticles. This is very difficult especially in the case of the heavy fermion systems. The effective mass and the band width contribute directly to the value of T_c, as Sasaki et $al.$ account for the difference of T_c for high-T_c cuprates of La system and that of Y system using the $d - p$ model.[28] Thus we have to adopt more realistic models such as the periodic Anderson model and calculate the higher order selfenergy corrections, to examine both the
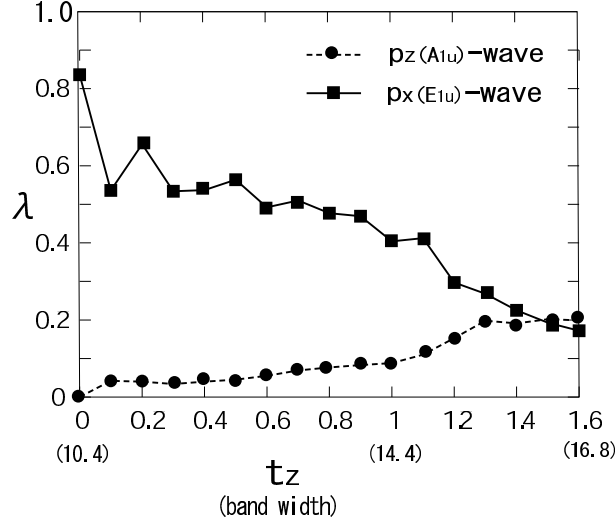
Fig. 12. The t_z-dependence of eigenvalues for p_z-wave (A_{1u}) pairing and p_x-wave (E_{1u}) pairing in the case of $t_2 = 0.3$, $t_3 = -0.5$, $n = 0.45$, $U = 9$ and $T = 0.01$. The solid (dashed) line with black squares (circles) is the result for p_x-wave (p_z-wave) in TOPT. The p_z-wave pairing stabilized by t_z is nearly degenerate with the suppressed p_x(or p_y)-wave in the region $1.3 \le t_z \le 1.5$.

heavy effective mass and T_c quantitatively.

Yamagami also calculated the energy band structure for UPt_3[29] using a fully-relativistic spin-polarized version of the linearized augmented-plane-wave (LAPW) method. The calculated energy band structure show us fact that, compered with the one we calculated in subsection 5.2, the six pockets are large and the main rugby ball like Fermi surface locates on the flat bottom of the dispersion. Thus, we have introduced further neighbor hopping integrals to reproduce his energy band structure and then calculated eigenvalues more precisely. However, the calculated density of state at the Fermi surface and the calculated T_c do not distinctly differ from those in subsection 5.2. Therfore, we do not miss the essence of band 37-electron using the simple Fermi surface calculated in subsection 5.2.

Our simple calculations predict the following points.

(1) The d-wave pairing is not possible because the antiferromagnetic fluctuation is suppressed.

(2) Only the triplt (odd parity) pairing is probable.

(3) Simple ferromagnetic fluctuation machanism can not explain the superconductivity of UPt_3. This is because the van Hove singularities and the small pocket structures exist only near the $k_z = 0$ plane.

(4) The p-wave pairing is the most probable. It is stabilized by the large vertex corrections from large U.

(5) The calculated T_c for p-wave pairing is rather low. In the renormalized scheme, the limit of the effective on-site repulsion is not clear because of the ambiguity of the band width of the

quasiparticles. In some case, we need to use larger value to realize the superconductivity of UPt_3.

7. Conclusion

In conclusion, on the basis of the microscopic theory, we have investigated the pairing symmetry and the transition temperture in the two-dimensional(2D) and three-dimensional(3D) hexagonal Hubbard model considering the band 37-electron in UPt_3. We have solved the Éliashberg equation using the third order perturbation theory with respect to U. As the results of the 2D calculation, we obtain distinct two types of stable spin-triplet pairing states. One is the f-wave(B_1) pairing in large filling n and small U region, which is caused by the ferromagnetic fluctuation. Then the other is the p_x(or p_y)-wave(E_1) pairing in large U region far from the half filling which is caused by the vertex corrections only. However, we find that the former f-wave pairing is easily destroyed by introduced 3D dispersion. This is because the 3D dispersion breaks the favorable structures for the f-wave pairing such as the van Hove singularities or the small pocket structures. Thus, the ferromagnetic fluctuation mediated spin-triplet state can not explain the superconductivity of UPt_3. We have also studied the case of pairing symmetry with a polar gap. This p_z-wave(A_1) is stabilized by both the large hopping integral along c-axis t_z and large U. It is nearly degenerate with the suppressed p_x(or p_y)-wave(E_1) in the best fitting parameter region to UPt_3 ($1.3 \leq t_z \leq 1.5$). The p_z-wave pairing partially agree with the experimental results. Finally, we note that these two p-wave pairing states exist far from the half-filling, in which the vertex correction terms play crucial roles like the case in Sr_2RuO_4.

Acknowledgements

References

1) G. R. Stewart, Z. Fisk, J. O. Willis and J. L. Smith: Phys. Rev. Lett. **52**(1984) 679.

2) R. A. Fisher, S. Kim, B. F. Woodfield, N. E. Phillips, L. Taillefer, K. Hasselbach, J. Flouquet, A. L. Giorgi and J. L. Smith: Phys. Rev. Lett. **62** (1989) 1411.

3) K. Hasselbach, L. Taillefer and J. Flouquet: Phys. Rev. Lett. **63** (1989) 93.

4) S. Adenwalla, S. W. Lin, Q. Z. Ran, Z. Zhao, J. B. Ketterson, J. A. Sauls, L. Taillefer, D. G. Hinks, M. Levy and Bimal K. Sarma: Phys. Rev. Lett. **65** (1990) 2298.

5) G. Aeppli, D. Bishop, C. Broholm, E. Bucher, K. Siemensmeyer, M. Steiner, and N. Stusser: Phys. Rev. Lett. **63** (1989) 676.

6) R. H. Heffner, D. W. Cooke, A. L. Giorgi, R. L. Hutson, M. E. Schillaci, H. D. Rempp, J. L. Smith, J. O. Willis, D. E. MacLaughlin, C. Boekema, R. L. Lichti, J. Oostens and A. B. Denison: Phys. Rev. B. **39** (1989) 11345.

7) B. S. Shivaram, Y. H. Jeong, T. F. Rosenbaum and D. G. Hinks: Phys. Rev. Lett. **56** (1986) 1078.

8) Y. Kohori, T. Kohara, H. Shibai, Y. Oda, T. Kaneko, Y. Kitaoka and K. Asayama: J. Phys. Soc. Jpn **56** (1987) 2263.

9) C. Broholm, G. Aeppli, R. N. Kleiman, D. R. Harshman, D. J. Bishop, E. Bucher, D. L. I. Williams, E. J. Ansaldo and R. H. Heffner: Phys. Rev. Lett. **65** (1990) 2062.

10) H. Tou, Y. Kitaoka, K. Asayama, N. Kimura, Y. Ōnuki, E. Yamamoto and K. Maezawa: Phys. Rev. Lett. **77** (1996) 1374.

11) G. M. Luke, L. P. Le, B. J. Sternlieb, W. D. Wu, Y. J. Uemura, J. H. Brewer, R. Kadono1, R. F. Kiefl, S. R. Kreitzman, T. M. Riseman, Y. Dalichaouch, B. W. Lee, M. B. Maple, C. L. Seaman, P. E. Armstrong, R. W. Ellis, Z. Fisk and J. L. Smith: Phys. Lett. A**157** (1991) 173.

12) R. Joynt, V. P. Mineev, G. E. Volovik, and M. E. Zhitomirsky: Phys. Rev. B **42** (1990) 2014.

13) J. A. Sauls: J. Low Temp. Phys. **95** (1994) 153.

14) K. Machida, T. Ohmi and M. Ozaki: J. Phys. Soc. Jpn. **62** (1993) 3216.

15) B. Lussier, B. Ellman and L. Taillefer: Phys. Rev. Lett. **73** (1994) 3294.

16) B. Lussier, B. Ellman and L. Taillefer: Phys. Rev. B **53** (1996) 5145.

17) T. Oguchi and A. J. Freeman: J. Magn. Magn. Matter. **52** (1985) 174.

18) M. R. Norman, R. C. Alberts, A. M. Boring and N. E. Christensen: Solid State Commun. **68** (1988) 245.

19) N. Kimura, R. Settai, Y. Ōnuki, H. Toshima, E. Yamamoto, K. Maezawa, H. Aoki and H. Harima: J. Phys. Soc. Jpn. **64** (1995) 3881.

20) N. Kimura, T. Komatsubara, D. Aoki, Y. Ōnuki, Y. Haga, E. Yamamoto, H. Aoki and H. Harima: J. Phys. Soc. Jpn. **67** (1998) 2185.

21) L. Taillefer and G. G. Lonzarich: Phys. Rev. Lett. **60** (1988) 1570.

22) K. Yamada and K. Yosida: Prog. Theor. Phys. **76** (1986) 621.

23) Y. Nisikawa, H. Ikeda and K. Yamada: J. Phys. Soc. Jpn. **71** (2002) 1140.

24) Y. Yanase, T. Jujo, T. Nomura, H. Ikeda, T. Hotta and K. Yamada: Phys. Rep. **387** (2004) 1.

25) T. Nomura and K. Yamada: J. Phys. Soc. Jpn. **72** (2003) 2053.

26) H. Ikeda, Y. Nisikawa and K. Yamada: J. Phys. Soc. Jpn. **73** (2004) 17.

27) H. Fukazawa and K. Yamada: J. Phys. Condens-Matter. **15** (2003) S2259.

28) S. Sasaki, H. Ikeda and K. Yamada: unpublished.

29) H. Yamagami: private communication.